Available online at www.sciencedirect.com
ScienceDirect
Biochimica et Biophysica Acta 1768 (2007) 39–51
Biochimica et Biophysica Acta BBA
www.elsevier.com/locate/bbamem

Gating of the ATP-sensitive K^+ channel by a pore-lining phenylalanine residue

Asheebo Rojas [1], Jianping Wu [1], Runping Wang, Chun Jiang*

Department of Biology, Georgia State University, 24 Peachtree Center Avenue, Atlanta, GA 30302-4010, USA

Received 17 April 2006; received in revised form 27 June 2006; accepted 28 June 2006
Available online 28 July 2006

Abstract

ATP-sensitive K^+ (K_{ATP}) channels are gated by intracellular ATP, proton and phospholipids. The pore-forming Kir6.2 subunit has all essential machineries for channel gating by these ligands. It is known that channel gating involves the inner helix bundle of crossing in which a phenylalanine residue (Phe168) is found in the TM2 at the narrowest region of the ion-conduction pathway in the Kir6.2. Here we present evidence that Phe168–Kir6.2 functions as an ATP- and proton-activated gate via steric hindrance and hydrophobic interactions. Site-specific mutations of Phe168 to a small amino acid resulted in losses of the ATP- and proton-dependent gating, whereas the channel gating was well maintained after mutation to a bulky tryptophan, supporting the steric hindrance effect. The steric hindrance effect, though necessary, was insufficient for the gating, as mutating Phe168 to a bulky hydrophilic residue severely compromised the channel gating. Single-channel kinetics of the F168W mutant resembled the wild-type channel. Small residues increased P_{open}, and displayed long-lasting closures and long-lasting openings. Kinetic modeling showed that these resulted from stabilization of the channel to open and long-lived closed states, suggesting that a bulky and hydrophobic residue may lower the energy barrier for the switch between channel openings and closures. Thus, it is likely that the Phe168 acts as not only a steric hindrance gate but also potentially a facilitator of gating transitions in the Kir6.2 channel.

Keywords: Kir6.2; K_{ATP} channel; Gating; Hydrophobicity; Steric hindrance

1. Introduction

ATP sensitive K^+ (K_{ATP}) channels are a special group of inward rectifier K^+ (Kir) channels whose activity is inhibited by physiological concentrations of ATP [1,2]. When the intracellular ATP level declines, the K_{ATP} channels open leading to hyperpolarization and a decrease in cellular excitability. Such a property enables these channels to couple the intermediary metabolism directly to cellular excitability. Indeed, the K_{ATP} channels are known to modulate a variety of cellular functions, including insulin secretion, cardiac rhythmicity, neuronal excitability, vascular tones, and skeletal muscle contractility [3–5]. The K_{ATP} channels are heteromeric consisting of four subunits of Kir6x and four subunits of sulphonylurea receptor (SURx). The Kir6x, that forms the ion-conduction pathway with two transmembrane domains, possesses the essential machineries for channel opening and closure controls [6]. Several cytosolic factors (ATP and H^+) and membrane phospholipids regulate the K_{ATP} channels by acting directly on the Kir6.2 subunit [1,7–10]. The channels are also regulated by ADP and sulfonylureas via the SUR subunits [11].

A central question in understanding the K_{ATP} channel function is how the channel opening and closure is produced following ligand binding, a process that is known as channel gating. Experimental evidence suggests that transmembrane domains, especially the pore-lining membrane helices, play an important role in the channel gating [12–14]. The Ca^{++}-dependent gating of the bacterial MthK channel occurs through lateral movements of the inner transmembrane helices (TM2) while the outer transmembrane domain (TM1) remains relatively rigid and stable [15]. Such TM2 helical movements during channel gating have also been implied in the KirBac1.1 and mammalian GIRK channels based on crystal structures

* Corresponding author. Tel.: +1 404 651 0913; fax: +1 404 651 2509.
E-mail address: cjiang@gsu.edu (C. Jiang).
[1] These authors contributed equally to this work.

0005-2736/$ - see front matter © 2006 Elsevier B.V. All rights reserved.
doi:10.1016/j.bbamem.2006.06.027

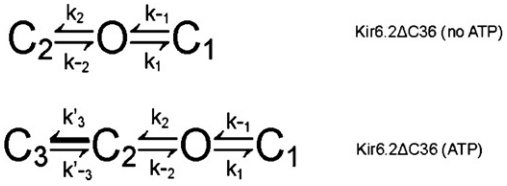

Scheme 1.

[16,17]. In the latter two Kir channels, a phenylalanine located at the narrowest region of the inner vestibule appears to play a critical role in the channel gating [16,17]. In Kir1.1 a leucine homologous to this phenylalanine was found to be essential for pH gating [18]. Such a phenylalanine residue (Phe168) is also found at the cytosolic end of the TM2 of the Kir6.2 subunit, which faces the ion-conduction pathway when its amino acid (AA) sequence is aligned with the KirBac1.1. Phenylalanine is hydrophobic with an aromatic side group. Recent studies on crystal structures of the bacterial mechanosensitive MscL channel, nicotinic acetylcholine receptor and the KirBac1.1 channel have indicated that nonpolar residues may form a gate through their hydrophobic interaction [17,19–21]. It is necessary to demonstrate that such a gate is not only a structural existence but also a functional entity. The functional role of Phe168 in Kir6.2 gating was investigated by replacing this residue with amino acids having side chains of different size and hydrophobicity. Our results suggest that the aromatic group of phenylalanine may occlude the ion conduction pathway in the closed state [16,17]. However, other residues with bulky or hydrophobic side chains at this location can also gate Kir6.2 in a similar manner. In addition to blockade of the ion pathway during the closed state, the Phe168 appears to lower the energy barrier necessary for the gating transition. Thus, this phenylalanine may act as a hinderer and a facilitator in the Kir6.2 channel gating.

2. Materials and methods

The Kir6.2 with a truncation of 36 AAs at the C-terminus end (Kir6.2ΔC36) expresses functional currents without the SUR subunit and retains ATP and pH sensitivities [6,10]. The Kir6.2ΔC36 and its mutants were subcloned to a eukaryotic expression vector (pcDNA3.1, Invitrogen Inc., Carlsbad, CA), and used for *Xenopus* oocyte expression without cRNA synthesis. Site-specific mutations were done using a site-directed mutagenesis kit (Stratagene, La Jolla, CA). Orientation of the correct mutations was confirmed with DNA sequencing.

Oocytes were surgically removed from adult female frogs (*Xenopus laevis*). The frogs were anesthetized by bathing them in 0.3% 3-aminobenzoic acid ethyl ester. A few lobes of ovaries were removed after a small abdominal incision (~5 mm). The surgical incision was then closed and the frogs were allowed to recover from the anesthesia. The *Xenopus* oocytes were treated with 2 mg/ml collagenase in the OR_2 solution containing: 82 mM NaCl, 2 mM KCl, 1 mM

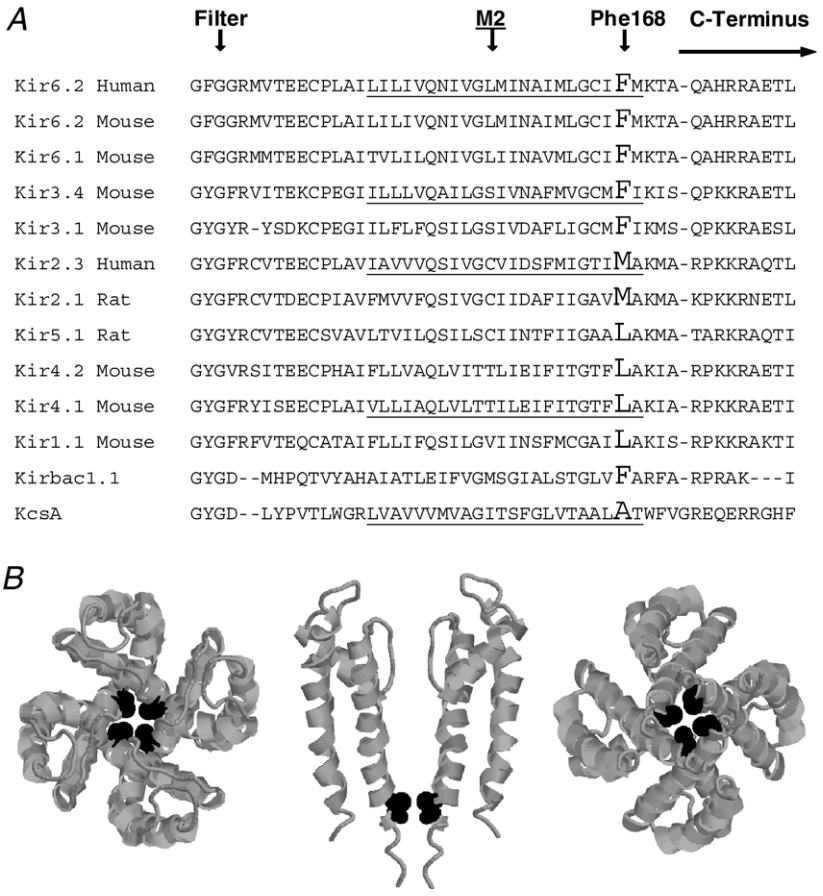

Fig. 1. (A) Alignment of the Kir6.2 with other K^+ channels in a region from the selectivity filter to the proximal C-terminus. (B) Phe168 is located in the narrowest sector of the inner pore when aligned with the KcsA sequence and viewed using RasMol modeling [39].

$MgCl_2$, and 5 mM HEPES with a titrated pH of 7.4. The eggs were digested at room temperature (~25 °C) for 90 min. After three washes (10 min each) of the oocytes with the OR_2 solution, cDNA in the pcDNA3.1 vector (25–50 ng in 50 nl of double distilled water) were injected into the oocytes. The oocytes were then placed in the ND-96 solution, which contains 96 mM NaCl, 2 mM KCl, 1 mM $MgCl_2$, 1.8 mM $CaCl_2$, HEPES 5 mM, sodium pyruvate 2.5 mM, and 100 mg/l Geneticin. This solution was also titrated to a pH of 7.4 and osmolarity of ~200 mosm/l. The cells were then incubated at 18 °C.

Whole cell currents were studied on the oocytes 2–4 days after injection using the two-electrode voltage-clamp at room temperature (~25 °C), as we described previously [10,22]. Expression of functional Kir channels were confirmed using one or two of the following methods: (1) the amplitude of the inward rectifying currents was significantly larger than that recorded from the pcDNA3.1-injected oocytes; (2) the currents were strongly activated with the exposure to 3 mM azide; and (3) 100 μM Ba^{++} inhibited the currents. When a mutant failed to express functional channels in ~60 oocytes tested, another two injections of the same mutant from different clones were followed in ~60 cells each. If there was still a lack of expression, we concluded that the mutation was probably too severe to produce any functional channels, and further experimentation was not attempted.

The pH-dependent channel gating was studied using CO_2 exposure [4,23,24]. In the experiments, the oocytes were placed in a semi-closed recording chamber on a supporting nylon mesh, where perfusion solution 90 K^+ (90 mM KCl, 3 mM $MgCl_2$, and HEPES) (pH 7.4) bathed both the top and bottom surfaces of the oocytes. The perfusate and superfusion gas (15% CO_2) entered the chamber from the inlet at one end and flowed out through the other end. At the top of the chamber, enough space was provided for the gases to escape and also for the recording microelectrodes to be injected into the oocytes. During baseline-control recording, the chamber was ventilated with atmospheric air. Exposure of the oocytes to CO_2 was carried out by exposing

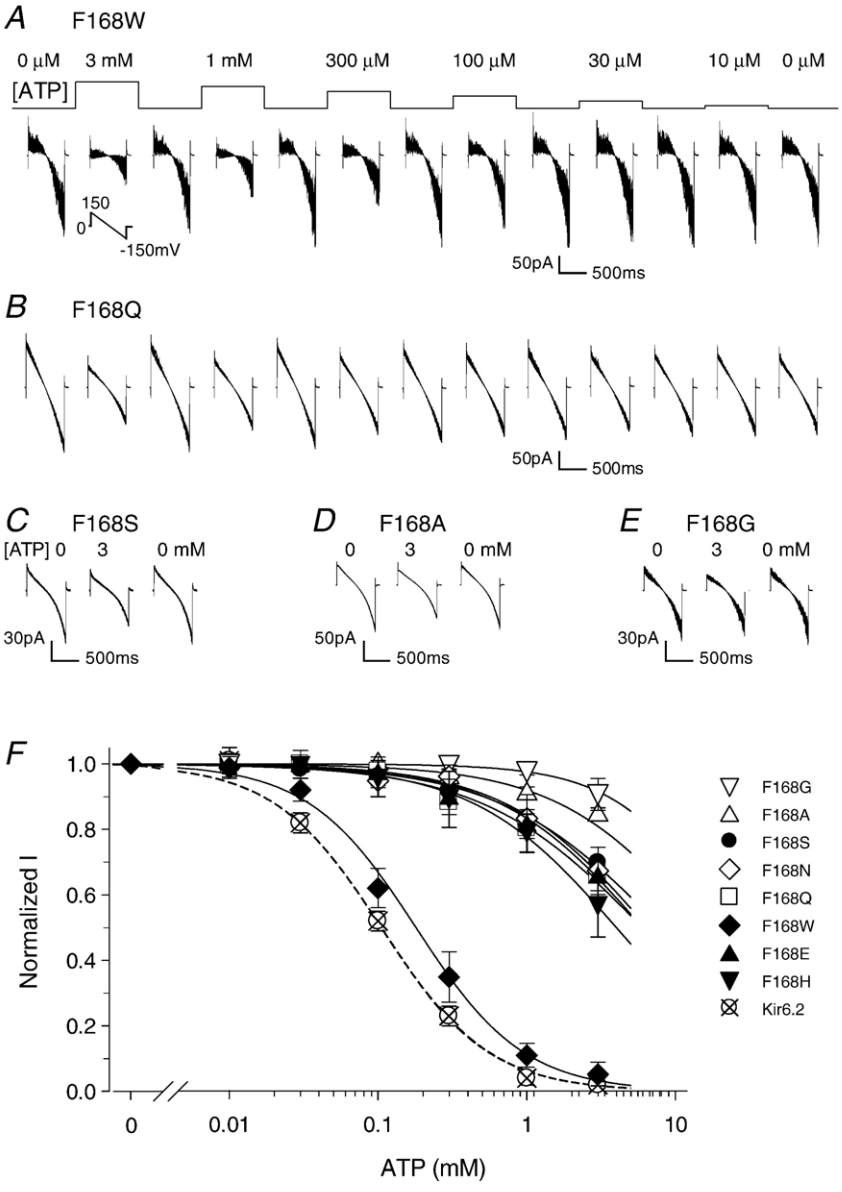

Fig. 2. ATP sensitivity of the Kir6.2 channel and its mutants. (A) Currents were recorded from an inside-out patch obtained from a cell expressing the Kir6.2ΔC36 F168W. With ramp potentials from −150 to 150 mV applied to the patch membrane inward rectifying currents were recorded. Exposures to ATP produced a dose-dependent inhibition of these currents with the ATP concentration for 50% current inhibition (IC_{50}) ~300 μM. (B) The Kir6.2ΔC36 F168Q mutant was only modestly inhibited by 1 mM ATP. Note that eight superimposed traces are shown in each panel. (C–E) The F168S, F168A, and F168G mutants of Kir6.2ΔC36 barely responded to 3 mM ATP. (F) The dose–response curves were produced using the Hill equation (see Materials and methods). All mutants were obtained from Kir6.2ΔC36. Data are presented as means±S.E. with IC_{50} shown in Table 1.

Table 1
Wild-type and mutant channels tested and their pH and ATP sensitivities

	IC_{50} ATP	% CO_2 effect	Baseline P_o	MW	Hydropathy[1]	Hydropathy[2]
F168G	>9000 (4)	4.5±3.8 (8)	0.052±0.004 (6)	75	−0.4	0.01
F168A	>9000 (4)	6.7±2.6 (9)	0.053±0.004 (6)	89	1.8	0.17
F168S	8061±1254 (6)	11.9±2.2 (7)	0.055±0.003 (4)	105	−0.8	0.13
F168V	NF	NF	NF	117	4.2	0.07
F168C	NF	NF	NF	121	2.5	−0.24
F168I	NF	NF	NF	131	4.5	−0.31
F168L	NF	NF	NF	131	3.8	−0.56
F168N	6562±797 (5)	15.8±4.0 (5)	0.050±0.005 (6)	132	−3.5	0.42
F168Q	6274±656 (4)	23.1±2.9 (10)	0.056±0.006 (13)	146	−3.5	0.58
F168K	NF	NF	NF	146	−3.9	0.99
F168E	5989±1441 (6)	−7.5±4.6 (6)	0.036±0.005 (4)	147	−3.5	2.02
F168M	NF	NF	NF	149	1.9	−0.23
F168H	4198±375 (4)	−24.6±3.4 (6)	0.046±0.005 (4)	155	−3.2	0.96
Kir6.2ΔC36	109±17 (14)	130.3±12.2 (9)	0.029±0.005 (7)	165	2.8	−1.13
F168R	NF	NF	NF	174	−4.5	0.81
F168Y	NF	NF	NF	181	−1.3	−0.94
F168W	195±24 (6)	150±16.6 (10)	0.039±0.003 (13)	204	−0.9	−1.85
*Kir6.2F168G	>9000 (6)		0.070±0.004 (5)			
*Kir6.2	7±0.6 (11)		0.169±0.014 (4)			
*Kir6.2F168W	13±2.6 (5)		0.243±0.016 (11)			

The ATP sensitivity was studied in excised patches and is expressed by fitting the data using the Hill equation. Hill coefficients are 1.0–1.2 (not shown). All mutants were created on Kir6.2ΔC36. Abbreviations: MW, molecular weight; NF, nonfunctional. Data are presented as means±S.E. with n (in the parentheses)=number of patches. Hydropathy was used to indicate whole-residue hydrophobicity according to the interface scale [40–42]. Hydropathy[1] refers to the Kyte–Doolittle hydropathy scale and hydropathy[2] refers to the White–Wimley scale. Asterisk indicates the channel expressed with SUR1.

the oocytes to a gas mixture containing 15% CO_2 balanced with 21% O_2 and N_2. The oocytes were exposed to this mixture for ~4–8 min or until the current reached a steady state. The high solubility of CO_2 resulted in very rapid changes in intracellular and extracellular pH levels. The pH level was stabilized within 4 min [10,23,24].

Patch clamp experiments were performed at room temperature (~25 °C) as described previously [10,22,25,]. In brief, fire-polished patch pipettes were made from 1.2 mm borosilicate glass capillaries using a Sutter P-97 puller (Sutter Instrument, Novato, CA). Giant inside-out patches were employed to study macroscopic currents in a cell-free condition using recording pipettes of 0.5–1.0 MΩ and an Axo-patch 200B amplifier (Axon Instruments, Foster City, CA). The current records were low-pass filtered (Bessel, 4-pole filter, −3 dB at 2 kHz), digitized with pClamp 9 software (Axon Instruments), and stored on computer disk for later data analysis. Patch clamp recording solutions contained equal concentrations of K^+ applied to the bath and recording pipettes. The solution contained (in mM): 10 KCl, 105 potassium gluconate, 5 KF, 5 potassium pyrophosphate, 0.1 sodium vanadate, 5 EGTA, 5 glucose, and 10 HEPES (pH=7.4) [10,22,25]. Pyrophosphate and vanadate are known to alleviate channel rundown. In several control experiments, we did not find any evident difference in current profile and channel responses to pH and ATP from those recorded in the absence of pyrophosphate and vanadate. The open-state probability (P_o) was calculated by measuring the time, t_j, spent at current levels corresponding to j=0,1,2,……N channels open, based on all evident openings during the entire period of record [22]. The P_o was then obtained as $P_o=(\sum^{N}_{j=1} t_j j)/TN$, where N is the number of channels active in the patch and T is the duration of recordings. Open and closed times were measured from records in which only a single channel was active. In the some patches, the second active channel appeared during recording. The data from such patches were used for the open-time and closed-time analysis only if the P_o for the second openings was not larger than 0.002. The open-time and closed-time distributions were fitted using the Marquardt-LSQ method in the Pstat6 software (Axon Instruments Inc.) [22]. Open/closed events <200 μs were ignored.

A parallel perfusion system was used to deliver perfusates with different concentrations of ATP (K^+ Salt) at a rate of ~1 ml/min with no dead space [10,25]. All solutions with ATP were prepared immediately before experiments and were used for less than 4 h. The ATP–current relationship was expressed with the Hill equation: $y=1/(1+([ATP]/IC_{50})^h)$, where [ATP]=ATP concentration, and IC_{50}=the [ATP] at midpoint channel inhibition. Data are presented as means±S.E. Differences in means were tested with the ANOVA or Student t test and accepted as significant if $P \le 0.05$.

Our data were fitted to the kinetic Scheme 1 in which O is the open state, C1 represents the short-lived closure, and C2 refers to the long-lived closed state in the absence of ATP. A third long-lived close state (C3) appears in the presence of ATP for the Kir6.2ΔC36. In the scheme the bold arrows indicate the transitions that are more favored and the dashed arrow refers to transitions that are lessened. The rate constants for Kir6.2ΔC36 were calculated from our single channel data based on the following equations: (Eqs. (1) Eqs. (2) Eqs. (3) Eqs. (4) Eqs. (5) Eqs. (6)) [26,27]:

$$\tau_{c1} = \frac{1}{k_{-1}} \quad (1)$$

$$\tau_{c2} = \frac{1}{k_{-2}} \quad (2)$$

$$\tau_{o} = \frac{1}{k_1 + k_2} \quad (3)$$

$$P_{OB} = \frac{1}{1 + \frac{k_1}{k_{-1}} + \frac{k_2}{k_{-2}}} \quad (4)$$

$$\tau_{c3'} = \frac{1}{k'_{-3}} \quad (5)$$

$$\tau_{c2'} = \frac{1}{k_{-2} + k_3'[ATP]} \quad (6)$$

$$P_{OB} = \frac{1}{1 + \frac{k_1}{k_{-1}} + \frac{k_2}{k_{-2}} + \frac{k_2 k_3}{k_{-2} k_{-3}}} \quad (7)$$

$$\frac{Nc_3}{Nc_1} = \frac{k_3 k_2}{k_1 k_{-2}} \quad (8)$$

$$\tau_{c2} = \frac{1}{k_{-2} + k_3} \quad (9)$$

$$\tau_{c3} = \frac{1}{k_{-3}} \quad (10)$$

where τc1 is the time constant for short closures, τc2 for long closures, τc3 for the additional long closures in the presence of ATP, and τ_o is the time constant for openings. P_{OB} is the open state probability in the absence of ATP. In the F168G mutant, an additional closed state appeared in the absence of ATP. Thus, additional equations (Eqs. (7) Eqs. (8) Eqs. (9) Eqs. (10)) were used to calculate the rate constant kinetics [26,27]. Under this condition τc3 is the additional long closed time constant, Nc3 and Nc1 are the number of C3 and C1 events. Notice that the equations used to calculate the F168G mutant are very similar to those used to calculate the kinetics of Kir6.2ΔC36. The difference is that the k_3 and k_{-3} in the F168G mutant represents the rate constant kinetics of the closed time in the baseline level (in the absence of ATP), which requires additional calculations.

3. Results

3.1. Phenylalanine 168 at the narrowest region of the ion conduction pathway

AA sequences of several mammalian Kir channels were aligned with sequences of the bacterial KirBac1.1 and KcsA channels in a region from the selectivity filter to the proximal C-terminus. Based on the crystallographic structures of KcsA and KirBac1.1, a phenylalanine is found at the narrowest region

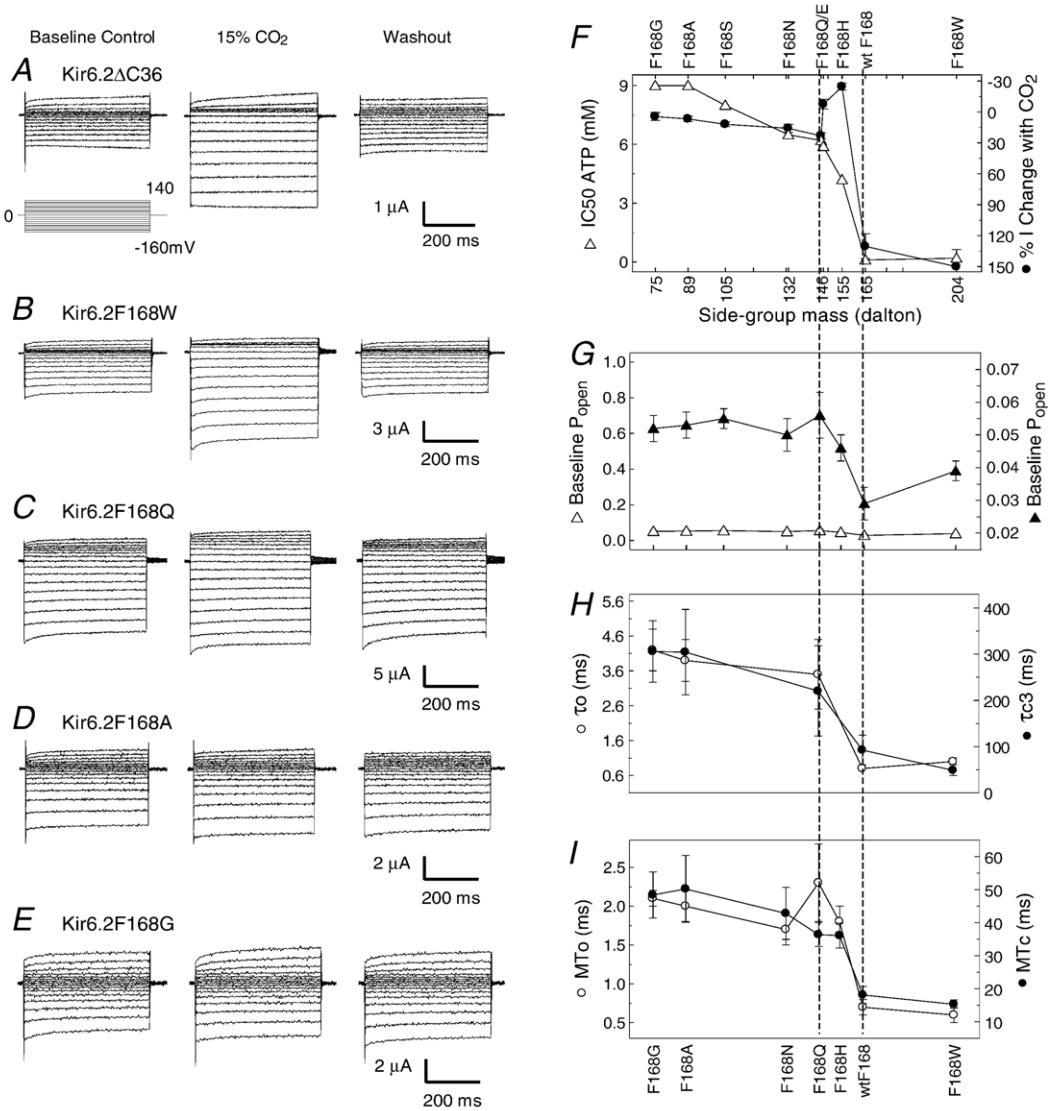

Fig. 3. (A) Activation of Kir6.2ΔC36 by hypercapnic acidosis. Whole-cell currents were studied in an oocyte injected with the Kir6.2ΔC36 3 days earlier. With 90 mM K^+ in the extracellular solution inward rectifying currents were recorded at baseline. The currents were reversibly activated with a 5 min exposure to 15% CO_2 that acidifies the cytosol to pH 6.6. (B) Mutation of Phe168 to tryptophan resulted in current activation similar to the Kir6.2ΔC36. (C) The channel was moderately activated when the Phe168 was mutated to glutamine. (D, E) Mutation to alanine or glycine yielded channels that were insensitive to CO_2. (F) The effects of ATP and CO_2 on single-channel and whole-cell currents were plotted against the residue mass [40] at the Phe168 location. A marked reduction in the pH and ATP sensitivities occurred with residues smaller than glutamine (146 Da). In contrast, the channels showed fair ATP and pH sensitivities with residue mass greater than 165 Da. When both plots were combined, the critical mass of this residue is shown to be >155 Da for the full ATP and pH sensitivities. Note that the channel response to acidic pH is inversely plotted. (G) The relationship of baseline P_o with residue mass. The P_o remained low no matter what AA the Phe168 was substituted with (open triangle). In higher magnification (solid triangle), the baseline P_o was significantly higher with small residues than with large ones with the transition between 145 and 165 Da. (H) The open-time constant (τ_o) and the long period of closed-time constant (τc3) obtained by fitting the dwell-time histogram as illustrated in Figs. 5–8 show a clear residue-mass dependence. Note that for comparison purpose, the open time was fitted with a single exponential for all channels. (I) Similar mass-dependence was observed with the mean open time (MT_o) and mean closed time (MT_c).

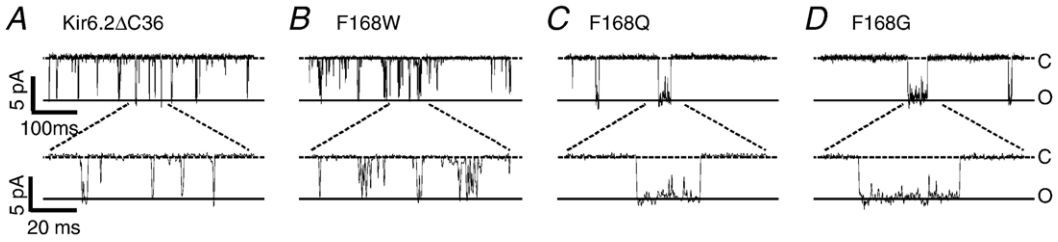

Fig. 4. Single-channel analysis of the open and closed times of the Kir6.2ΔC36 and its representative mutants. (A–D) The Kir6.2ΔC36 and F168W show brief openings and closures, while the openings and closures are much longer in F168G and F168Q. Labels on the right indicate the opening (o) and closure levels (c).

of the inner vestibule of the ion-conduction pathway in the Kir6 and Kir3 subfamilies (Fig. 1A, also see ref. [18]). These Kir channels have rather low basal channel activity. A hydrophobic residue with an intermediate size side group (Leucine, methionine) is also seen in other Kir channels, most of which show high baseline P_o. Based on the crystal structure of the KirBac1.1 and KcsA channels [17,28], the phenylalanine residue faces the pore with its side chain projecting into the ion pathway (Fig. 1B).

3.2. ATP- and H^+-dependent channel gating with different residue mass and hydrophobicity at position 168

Site-specific mutations of the Phe168 to small amino acids (alanine, glycine or serine) allowed expression of functional inward rectifying currents. However, these mutations severely disrupted the channel gating by intracellular ATP. The mutant channels barely responded to 3 mM ATP, whereas the wild-type Kir6.2ΔC36 channel was strongly inhibited by micromolar concentrations of ATP (Figs. 2C–E, F). In contrast to these mutations, the ATP-dependent channel gating was well maintained when the Phe168 was mutated to a bulky tryptophan (Fig. 2A). The F168W mutant showed a similar ATP sensitivity as the wild-type channel (Figs. 2F, 3F), suggesting that a bulky amino acid is necessary for the ATP-dependent channel gating. Slightly smaller than phenylalanine, histidine is a hydrophilic amino acid with a bulky side chain. The F168H mutation produced a channel that was poorly gated by intracellular ATP (Fig. 2F), suggesting that the residue mass is not the only player in the Kir6.2 channel gating, and hydrophobicity is also important. Further supporting this idea was that mutant channels carrying a hydrophilic amino acid (i.e., glutamine, asparagine, glutamate) at residue 168 were also poorly gated by ATP (Fig. 2F, Table 1). Mutations to other massive and hydrophilic residues (tyrosine, arginine) did not yield functional channels. The similar phenomenon was observed in the presence of the sulphonylurea receptor 1 subunit (SUR1). In the presence of SUR1 the 168 position showed a size dependent effect similar to the Kir6.2ΔC36. The presence of the SUR1 increased the channel sensitivity to ATP without affecting the gating mechanism (Online Fig. 1, Table 1).

The same gating pattern was observed for the proton-dependent gating of the Kir6.2. The F168A and F168G mutations greatly diminished or completely eliminated the channel gating by pH (Fig. 3D–F). The pH sensitivity was well maintained when the Phe168 was mutated to a bulky tryptophan (Fig. 3B). Mutation to an AA with a medium side-chain (glutamine, asparagine) had an intermediate effect (Figs. 3C, F), while mutation to glutamate or histidine reversed the pH response (Table 1).

When the ATP and pH sensitivities were plotted against the residue mass, we found that the effect of ATP and pH on channel activity was a function of the residue mass (Fig. 3F). With a residue of 165 Da or larger, the channels were fully functional. They were strongly activated by protons and inhibited by ATP, whereas mutations to a residue

Table 2
Single channel data of wild-type and representative mutant channels

	F168G	F168Q	Kir6.2ΔC36 F168	F168W
pH7.4, no ATP				
P_o	0.049±0.003 (17)	0.056±0.007 (14)	0.029±0.004 (7)	0.039±0.004 (9)
MT_o	2.1±0.1 ms (11)	2.3±0.5 ms (14)	0.7±0.1 ms (6)	0.6±0.1 ms (9)
MT_c	48.4±7.0 ms (11)	36.4±3.6 ms (14)	18.1±2.6 ms (6)	15.3±1.3 ms (9)
pH7.4, 100 μM ATP				
P_o	–	–	0.008±0.002 (4)	0.021±0.002 (4)
MT_o	–	–	0.8±0.0 ms (4)	0.6±0.0 ms (4)
MT_c	–	–	67.1±4.3 ms (4)	22.4±2.7 ms (5)
pH7.4, 1 mM ATP				
P_o	0.047±0.008 (7)	0.040±0.007 (6)	–	–
MT_o	2.6±0.3 ms (7)	2.7±0.5 ms (6)	–	–
MT_c	60.2±7.6 ms (7)	64.0±7.5 ms (6)	–	–

The open-state probability (P_o), mean open time (MT_o), and mean closed time (MT_c) were studied in patches with a single active channel. Excised inside-out patches were exposed to 100 μM ATP or 1 mM ATP as dependent upon the IC_{50} of the mutant and compared to controls with no ATP. All mutants were based on the Kir6.2ΔC36. Data are presented as means±S.E. with *n* shown in parentheses and represents the number of patches.

Table 3
Rate constants used for kinetic modeling

	Kir6.2ΔC36	Kir6.2ΔC36–F168G
τo1	0.6	4.2
τc1	0.2	0.3
τc2	38.0	2.5
τc3		255.6
τc2′	27.4	
τc3′	197.3	
k_1	720.2	162.1
k_{-1}	4,545.4	4000.0
k_2	1065.5	76.0
k_{-2}	26.3	257.5
k_3		138.5
k_{-3}		3.9
k'_3	102,230.0	
k'_{-3}	5.1	

The average rate constants were calculated at −80 mV. The τc2′, τc3′, k'_3 and k'_{-3} were obtained in the presence of 100 μM ATP.

smaller than glutamine (146 Da) disrupted the channel gating by both ATP and pH. The transition occurs between 146 and 165 Da (Fig. 3F), suggesting that residue mass at this location is critical for the Kir6.2 channel gating.

To understand whether the hydrophobic nature of phenylalanine is adequate for the channel gating, we also studied mutant channels with several other nonpolar amino acids such as valine, leucine, isoleucine and methionine at residue 168. None of these mutants produced detectable K^+ currents (Table 1).

3.3. Effects of residue mass and hydrophobicity on the single channel properties

Consistent with previous reports [6,22], single-channel Kir6.2ΔC36 currents showed short periods of openings with low baseline P_o (Fig. 4, Table 2). The F168W-mutant channel showed similar single-channel activity with moderate bursting activity (Fig. 6). It is worth noting that the F168W channel did not show rapid rundown. With a small residue at this position, the F168G channel had much longer openings and closures than the Kir6.2ΔC36 (Figs. 4, 7), leading to a marked decrease in the closure-opening frequency. These mutant channels ran down rather fast in contrast to the F168W, especially when the patches were exposed to acidic pH that causes rundown in wild-type Kir6.2 as well, though to a lesser degree [10,25].

Although the baseline P_o of all mutant channels remained low (Table 1), significant differences in the baseline P_o was observed between large and small residues. The baseline P_o of the F168G was almost twice as high as the Kir6.2ΔC36 ($P<0.01$), despite the fact that its rapid rundown may have led to an under-estimation of the P_o value. When the residue mass was plotted against P_o, a clear transition of P_o levels was also seen at the residue mass of 146–165 Da (Fig. 3G). We also examined the channel open- and closed-time properties and when plotted, the residue-mass dependence was observed in these open and closed time properties with a transition at 146–165 Da (Fig. 3H, I).

3.4. Mutations at position 168 in Kir6.2 also affect single-channel kinetics

Channel open-time and closed-time properties were studied on the F168W, F168Q and F168G mutants that represent residues of different size and hydrophobicity (Figs. 6–8). The open time constant (τ_o) and the mean open time (MT_o) of the F168W were comparable to those of Kir6.2ΔC36 (Table 2, Table 4), although its bursting activity caused a reduction in long periods of closures leading to a modest decrease in the closed-time constants (τ_c) and the mean closed time (TM_c) (Table 2). The F168G and F168Q channels all showed much longer openings and closures (Table 2). They also had longer τ_o and τ_c as well as longer MT_o and MT_c (Table 2, Table 4). Thus the mutant channels without a bulky and hydrophobic residue at the 168 position tend to stay in long periods of openings and closures (Fig. 4C, D), strongly suggesting that the Phe168 is not only involved in blocking the ion pathway by its bulky side-group, but also facilitates the transition between channel openings and closures.

Like Kir6.2ΔC36 (Fig. 5), the F168W channel was fairly sensitive to ATP. The inhibition by ATP was produced by selective augmentation of the long closures with little or no effect on the openings (Fig. 6D, E). This led to an increase in the MT_c with little effect on the MT_o (Table 2). The F168G mutant was unaffected by ATP up to 3 mM ATP. As a result, there were no evident changes in its single-channel kinetics with 1 mM ATP (Fig. 7, Table 4). The F168Q was modestly inhibited by ATP. Such a small effect was also mediated by changes in the closed time constants (Fig. 8). Taken together, these results suggest that the mechanism for ATP inhibition remains similar

Table 4
Open and closed time constants for wild-type and mutant channels

	Kir6.2ΔC36	Kir6.2ΔC36–F168W	Kir6.2ΔC36–F168Q	Kir6.2ΔC36–F168G
τo1	0.56±0.04 (5)	0.5±0.06 (5)	3.5±1.0 (5)	4.2±0.55 (4)
τc1	0.22±0.02 (5)	0.3±0.0 (5)	0.3±0.1 (5)	0.3±0.03 (4)
τc2	38.02±11.18 (5)	17.86±2.72 (5)	10±2.4 (5)	2.5±0.74 (4)
τc3			162.2±74.2 (5)	255.55±79.65 (4)
*τo1	0.68±0.066 (5)	0.95±0.1 (4)	4.0±0.7 (5)	4.2±0.6 (4)
*τc1	0.3±0.05 (5)	0.65±0.06 (4)	0.4±0.0 (5)	0.3±0 (4)
*τc2	27.38±12.83 (5)	14.13±2.76 (4)	13.8±2.1 (5)	2.9±0.8 (4)
*τc3	197.26±84.55 (5)	94.53±25.16 (4)	240.5±64.4 (5)	254.9±78.7 (4)

The open time constant (τo1) and the closed time constants (τc1, τc2, τc3) were studied in patches with a single active channel. Excised inside-out patches were exposed to 100 μM ATP or 1 mM ATP as dependent upon the IC_{50} of the mutant and compared to controls with no ATP. All mutants were based on the Kir6.2ΔC36. Data are presented as means±S.E. with *n* shown in parentheses and represents the number of patches. Asterisk represents data obtained in the presence of ATP.

in the F168W and F168Q mutants although the magnitude of the inhibition is different.

3.5. Kinetics modeling

The rate constant kinetics was determined for the Kir6.2ΔC36 in the basal condition as well as in the presence of ATP [26,27]. We adopted a simple kinetic scheme used previously for the K_{ATP} channel [27]. In an ATP-free condition, the Kir6.2ΔC36 channel has a single O with C1, and C2. The C1 is the short-lived closed state that can be seen in bursts of openings, and C2 is the long-lived closed state that determines the duration between bursts. During baseline levels the Kir6.2ΔC36 channel exhibits bursting that is reflective in the rate time kinetics (Table 1). This channel tends to have alternating fast and slow kinetics between open and closed states. The scheme is supported by the rate constant kinetics calculated based on the equations described in the methods section. The kinetic model suggests that the Kir6.2ΔC36 channel spends very little time in either the closed or open states. The transitions between the states are very rapid. During channel opening there is a fast transition to the short-lived closed state. In the absence of ATP the kinetics favors a very fast transition from the short-lived closure to the open state and also a very fast transition from the open state to the long-lived closed state. This explains why in the basal condition this channel exhibits bursting or flickering activity. When ATP is present, a second long-lived closed state (C3) appears in the Kir6.2ΔC36 (Scheme 1). The kinetics favors a very fast transition towards C3 in the presence of ATP as indicated by the bold arrow. As a result the C2 is shortened by ATP. Therefore, ATP inhibits the channel by extending the long-lived closed state.

To determine whether the Phe168 is critical for this gating transition, we calculated the rate constant kinetics for the F168G mutant that causes severe disruption of channel gating, and compared them with the rate constant kinetics of the Kir6.2ΔC36. The data for the F168G was fitted with the kinetic Scheme 2. When the kinetics was entered into the

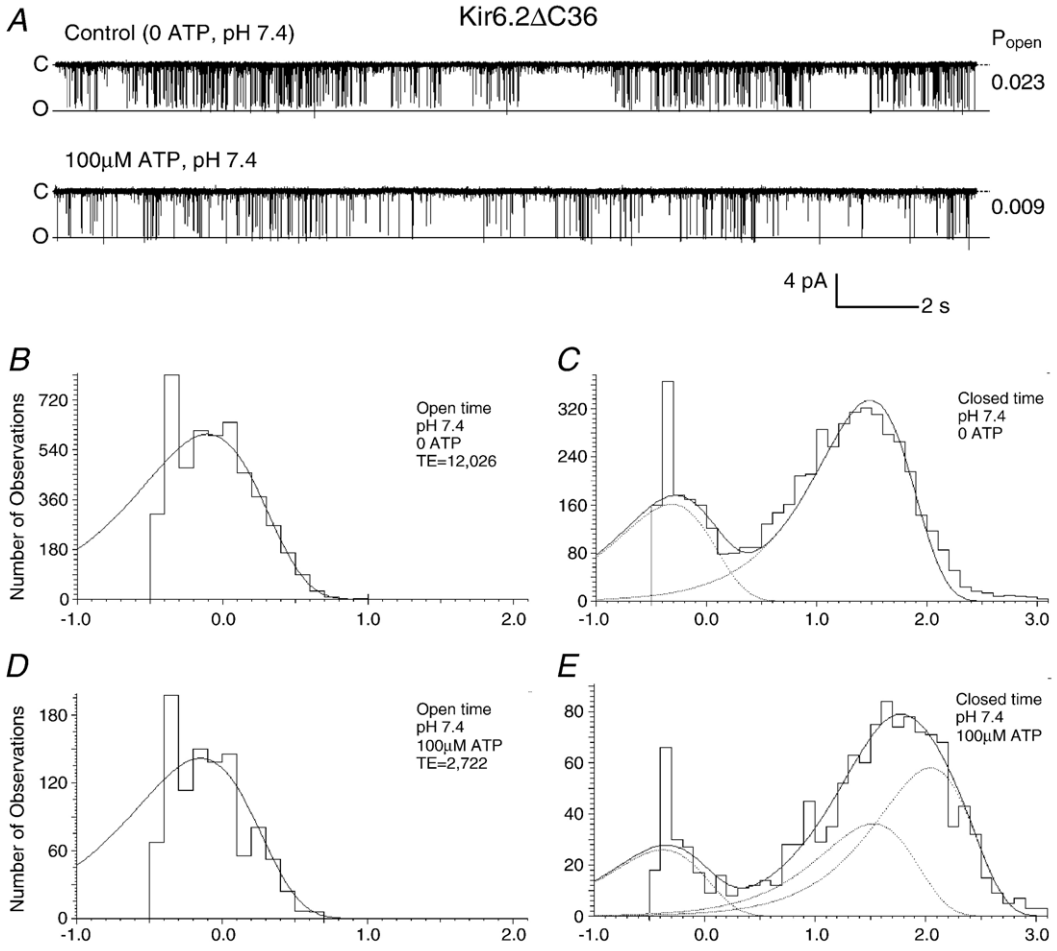

Fig. 5. Single-channel kinetics analysis of the Kir6.2ΔC36 channel. Data were obtained from an inside-out patch with each histogram constructed using >1 min recording. (A) Single-channel current recorded from the patch was studied with different levels of ATP. Channel activity (P_o, shown on the right) decreased in the presence of 100 μM ATP (lower trace). Labels on the left indicate the opening (o) and closure levels (c). The total number of events (TE) used to compute the histogram is also in the caption. (B, C) Baseline open-time and closed-time histograms at pH 7.4 in the absence of ATP. (B) The open-time histogram was fitted with one exponential with $\tau_o = 0.7$ ms. (C) The closed time was fitted with two exponentials with $\tau c1 = 0.3$ ms and $\tau c2 = 28.8$ ms. (D, E) In the presence of 100 μM ATP (pH 7.4), a third closure event appeared and was very long. The time constant for the second closure was slightly changed, but the third closure was prolonged ($\tau c2 = 33.7$ ms, $\tau c3 = 110.9$ ms), while the other time constants were barely affected.

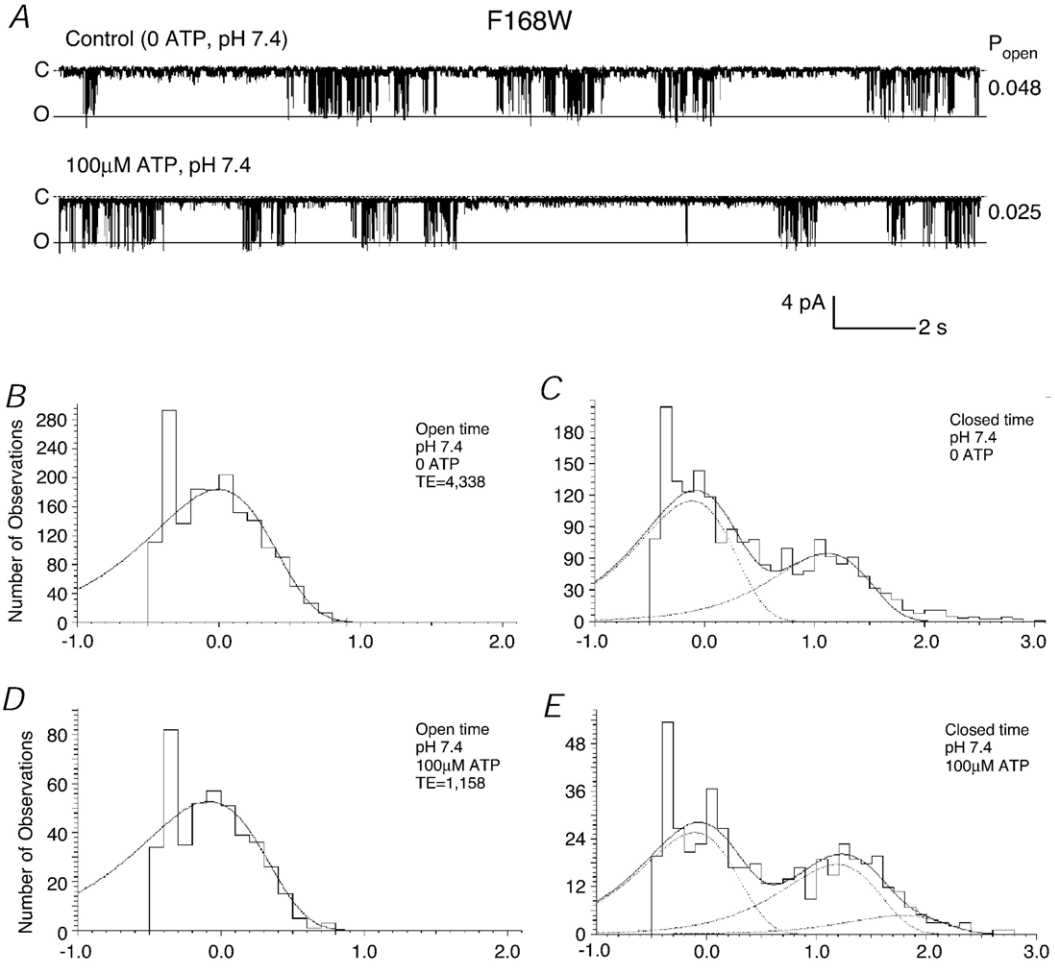

Fig. 6. Single-channel kinetics analysis of F168W. Data were obtained from an inside-out patch with each histogram constructed using two stretches of 20 s recording in B and C and one stretch in D and E. (A) Single-channel current recorded from the patch was studied with different levels of ATP. Channel activity (P_o, shown on the right) decreased in the presence of 100 μM ATP (lower trace). Labels on the left indicate the opening (o) and closure levels (c). The total number of events (TE) used to compute the histogram is also in the caption. (B, C) Baseline open and closed time histograms at pH 7.4 in the absence of ATP. (B) The open time histogram was fitted with one exponential with $\tau_o = 1.0$ ms. (C) The closed time was fitted with two exponentials with $\tau c1 = 0.8$ ms and $\tau c2 = 13.1$ ms. (D, E) In the presence of 100 μM ATP (pH 7.4), time constants for the second closure changed a little and a third closures became apparent and was long ($\tau c2 = 15.4$ ms, $\tau c3 = 60.3$ ms), while the other time constants were barely affected.

scheme it supported the idea that the F168G mutation has an increased barrier of energy necessary for the gating transitions. The rate constant kinetics for this mutant favors the transition towards openings from both C1 and C2 allowing the channel to stay in the open state (Table 3). The transition from open to C1 is lessened as noted by the dashed arrow (Table 3). Furthermore, the kinetics also favors the transition from C2 to C3 stabilizing at the long-lived close state (Table 3). Therefore, the F168G mutant unlike the Kir6.2ΔC36 has long periods of closures followed by long periods of openings. This results in the slow transition between channel opening and closure, a completely opposite effect to the bursting activity seen in the Kir6.2ΔC36.

4. Discussion

Our results have shown that a bulky and hydrophobic AA is required at residue 168 for the Kir6.2 channel gating. With a small residue at this site, the mutant channels remain conducting inward rectifying K^+ currents, but fail to be gated by ATP and protons. The requirement of a bulky residue on the ion-conduction pathway for channel gating therefore suggests a steric hindrance effect. In addition to the residue-mass dependence, hydrophobicity of residue 168 is important for the Kir6.2 channel gating. The size of the residue at position 168 cannot completely account for full channel gating. Various side chain characteristics may contribute to the gating properties. This is apparent in channels carrying charges at the 168 position such as F168E and F168H. These two channels show disrupted pH gating which may attribute to the charge carried by these amino acids. The Kir6.2 channel is well gated with a hydrophobic but not a hydrophilic residue. These results are consistent to what has been reported for the pH gating of Kir1.1 [18].

Based on crystal structures of the bacterial mechanosensitive MscL channel, nicotinic acetylcholine receptor and the KirBac1.1 channel, a hydrophobic residue is often found at the narrowest region of the ion-conduction pathways [17,19–

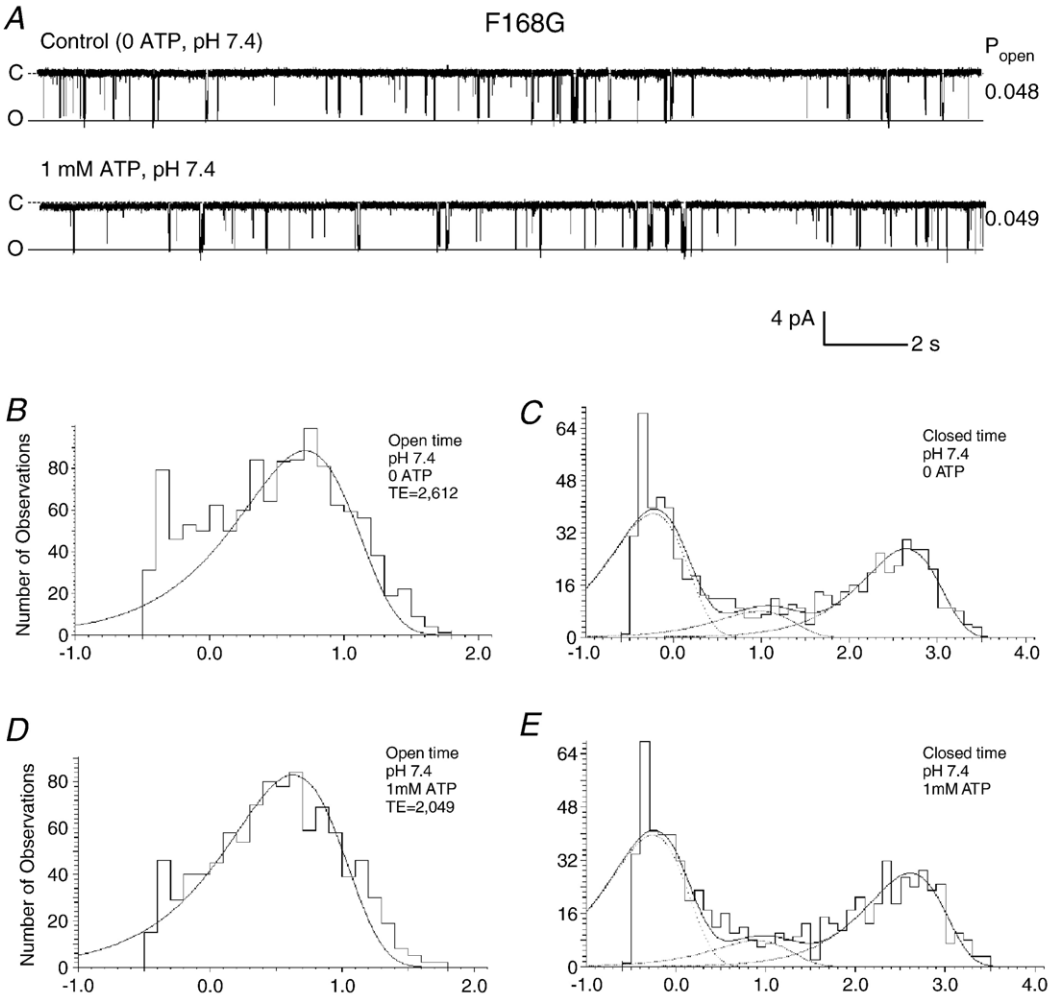

Fig. 7. Single-channel kinetics analysis of F168G. Data were obtained from an inside-out patch with each histogram constructed using ≥1 min recordings. (A) Single-channel current recorded from the patch was studied with different levels of ATP. Channel activity (P_o, shown on the right) was unaffected in the presence of 1 mM ATP (lower trace). Labels on the left indicate the opening (o) and closure levels (c). The total number of events (TE) used to compute the histogram is also in the caption. (B, C) Baseline open and closed time histograms at pH 7.4 in the absence of ATP. (B) The open time histogram was fitted with one exponential with $\tau o1 = 5.14$ ms. (C) The closed time was fitted with three exponentials with $\tau c1 = 0.6$ ms, $\tau c2 = 9.6$ ms, $\tau c3 = 437.9$ ms. (D, E) ATP (1 mM, pH 7.4) had no effect on the time constants ($\tau c1 = 0.5$ ms, $\tau c2 = 7.9$ ms, $\tau c3 = 407.9$ ms).

21], leading to the "hydrophobic gate" hypothesis: Gating of these channels involves movements of the pore-lining helices with the pore widened during channel opening, while constriction of these pore-lining helices during channel closure brings the nonpolar residues in each subunit of a multimeric channel in contact with each other, thereby sealing the ion-conduction pathway [13]. Our studies have evaluated this hypothesis by looking at functional consequences of different amino acid properties at residue 168. Our results have shown that a hydrophobic residue is necessary for the Kir6.2 channel gating. The channel gating is severely compromised when the Phe168 is mutated to a hydrophilic amino acid including histidine that has almost the same residue mass as phenylalanine. Thus, these results provide functional evidence supporting the hydrophobic gate hypothesis (Table 4).

Phenylalanine has an aromatic side group. According to the KirBac1.1 model [17], the Phe168 faces the pore and may block the ion-conduction pathway by the bulky side group (Online Fig. 2). The involvement of such a phenylalanine residue in channel gating has been suggested in KirBac1.1 and GIRK channels. In the GIRK4 channel, Phe187 is located at the narrowest part of the ion-conduction pathway. The channel gating requires flexibility of the TM2 helix above the Phe187, while introduction of flexibility at the helical turn below the Phe187 renders the TM2 helix unable to transduce the force exerted at its end by the channel-G-protein interaction and fails to produce functional channels [16]. In the KirBac1.1 channel, a phenylalanine (Phe146) is identified at the corresponding site to the Phe187 in GIRK4 and Phe168 in Kir6.2. Side chains of the Phe146 have been shown to form structural obstacles in the ion-conduction pathway in the closed state [17]. Similarly, leucine residues at a homologous position on Kir1.1 occlude the permeation path of Kir1.1 in the closed state [18]. According to the White–Wimley hydropathy scale [41,42], leucine is more hydrophobic than its counterpart isoleucine and valine, suggesting that this

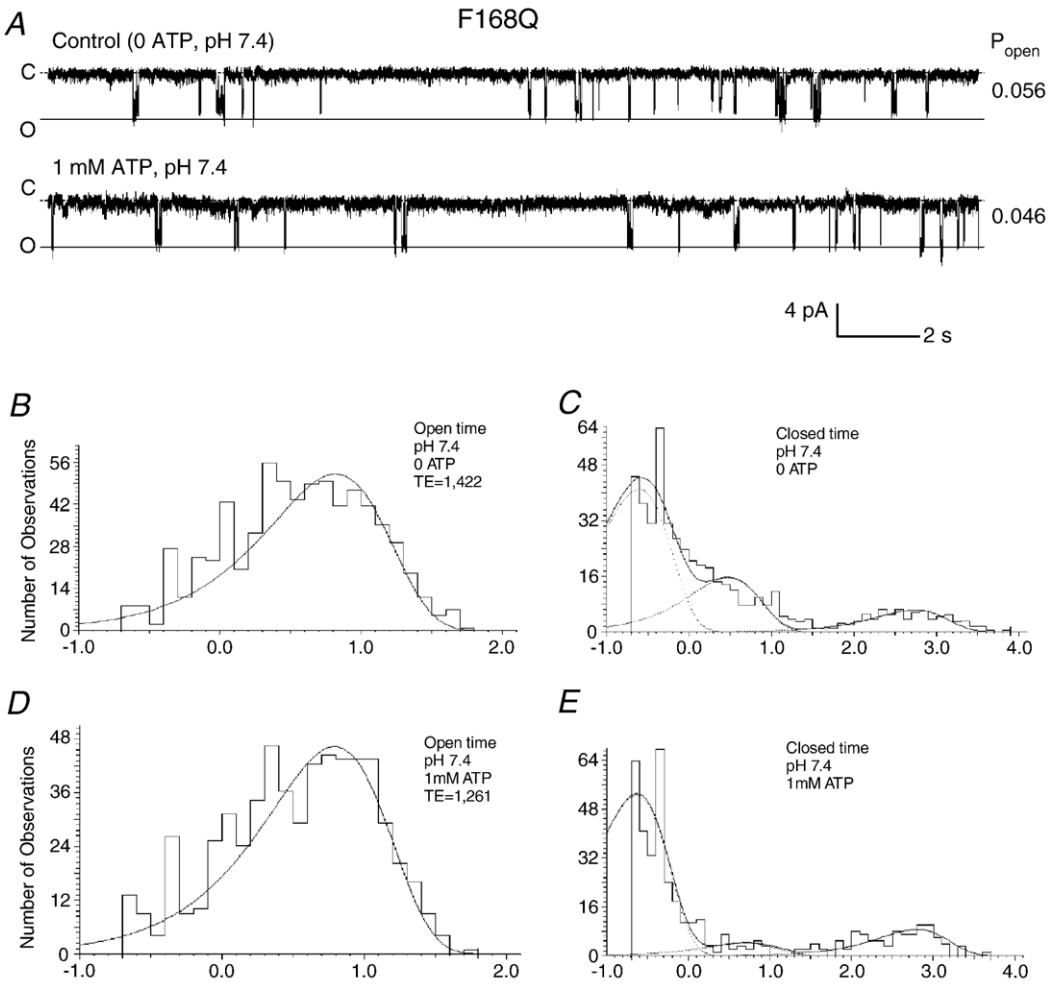

Fig. 8. Single-channel kinetics analysis of F168Q. Data were obtained from an inside-out patch with each histogram constructed using ≥1 min recordings. (A) Single-channel current recorded from the patch was studied with different levels of ATP. Channel activity (P_o, shown on the right) decreased in the presence of 1 mM ATP (lower trace). Labels on the left indicate the opening (o) and closure levels (c). The total number of events (TE) used to compute the histogram is also in the caption. (B, C) Baseline open and closed time histograms at pH 7.4 in the absence of ATP. (B) The open time histogram was fitted with one exponential with $\tau o1 = 6.6$ ms. (C) The closed time was fitted with three exponentials with $\tau c1 = 0.2$ ms, $\tau c2 = 3.0$ ms, $\tau c3 = 563.6$ ms. (D, E) In the presence of 1 mM ATP (pH 7.4), time constants for the second and third closures were slightly prolonged ($\tau c1 = 0.2$ ms, $\tau c2 = 5.0$ ms, $\tau c3 = 640.0$ ms), while the other time constants were barely affected.

leucine residue in the Kir1.1 channel may act similarly as Phe168 in the Kir6.2 channel.

In Kir6.2, the baseline channel openings are maintained by the intrinsic conformation of the channel protein, phosphorylation and other K_{ATP} channel regulators such as phospholipids, ADP and protons [7,8,10,22,29,30]. ATP binding to intracellular protein domains [31,32] may produce a conformational change of the inner helices. When the phenylalanine from each subunit are close enough, they can interact with each other through hydrophobic forces and close the ion pathway (Online Fig. 2), as indicated in the KirBac1.1 crystallographic structure [17]. Substitution of this Phe168 residue with a smaller amino acid eliminates the gating ring, and disrupts the channel gating.

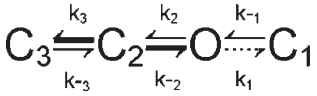

Scheme 2.

The pore blockade may be removed during channel opening, as it is known that the inner helix bundle-crossing moves and the inner pore is widened with channel opening [9,15,33–38], suggesting that the Phe168 also acts on the channel gating by the steric hindrance effect.

A kinetic model is helpful to understand how this phenylalanine can have this steric hindrance effect. We thus used the simplest kinetic scheme to explain our data for the Kir6.2ΔC36 and the F168G mutant channels. In the basal condition, the Kir6.2ΔC36 channel contains two close states (C1, C2) and one open state (O). A third long-lived closed state appears when ATP is present in the solution. In contrast to the Kir6.2ΔC36, the F168G mutant contains one open state and three closed states (C1, C2, C3) in the absence of ATP. The C1 and C2 are similar to those in the Kir6.2ΔC36, while the C3 is a long-lived closed state independent of ATP. Kinetic analysis shows that the F168G mutant tends to be stabilized in the open and long-lived closed states. Under such a condition, higher free energy is needed to fulfill the gating transitions.

This is consistent with the observation that this mutant channel is no longer sensitive to ATP concentrations that strongly inhibit the Kir6.2ΔC36. The mere presence of a phenylalanine at position 168 in the Kir6.2ΔC36 appears sufficient to lower the barrier of energy necessary for the gating transitions. In this respect, phenylalanine is likely to act as a facilitator of the channel gating. Thus, a bulky and hydrophobic residue like phenylalanine and tryptophan may block the ion-conduction pathway in the closed state and facilitate the closure-opening transition in channel gating. Apparently this is a consequence of evolutionary optimization of protein function. This phenylalanine is not seen in several other Kir channels including Kir1.1, Kir2.1 and Kir4.1. Instead, a leucine or methionine is found in those channels. It is known that some of these hydrophobic residues with an intermediate side chain also serve as a gate as is the case in the Kir1.1 channel [18]. Under such a condition, a reduced hydrophobicity of the pore-lining residues may be necessary for preventing pore collapse or channel rundown.

Acknowledgments

Special thanks to Dr. S. Seino at Chiba University in Japan and Dr. J. Bryan at Baylor University in the USA for the gifts of Kir6.2 and SUR1 cDNAs, respectively. This work was supported by the NIH (HL067890).

Appendix A. Supplementary data

Supplementary data associated with this article can be found, in the online version, at doi:10.1016/j.bbamem.2006.06.027.

References

[1] A. Noma, ATP-regulated K^+ channels in cardiac muscle, Nature 305 (1983) 147–148.
[2] D.L. Cook, C.N. Hales, Intracellular ATP directly blocks K^+ channels in pancreatic B-cells, Nature 311 (1984) 271–273.
[3] F.M. Ashcroft, Adenosine 5′-triphosphate-sensitive potassium channels, Annu. Rev. Neurosci. 11 (1988) 97–118.
[4] F.M. Ashcroft, F.M. Gribble, ATP-sensitive K^+ channels and insulin secretion: their role in health and disease, Diabetologia 42 (1999) 903–919.
[5] C.G. Nichols, A.N. Lopatin, Inward rectifier potassium channels, Annu. Rev. Physiol. 59 (1997) 171–191.
[6] S.J. Tucker, F.M. Gribble, C. Zhao, S. Trapp, F.M. Ashcroft, Truncation of Kir6.2 produces ATP-sensitive K^+ channels in the absence of the sulphonylurea receptor, Nature 387 (1997) 179–183.
[7] T. Baukrowitz, U. Schulte, D. Oliver, S. Herlitze, T. Krauter, S.J. Tucker, J.P. Ruppersberg, B. Fakler, PIP2 and PIP as determinants for ATP inhibition of K_{ATP} channels, Science 282 (1998) 1141–1144.
[8] S.L. Shyng, C.G. Nichols, Membrane phospholipid control of nucleotide sensitivity of KATP channels, Science 282 (1998) 1138–1141.
[9] N.W. Davies, Modulation of ATP-sensitive K^+ channels in skeletal muscle by intracellular protons, Nature 343 (1990) 375–377.
[10] H. Xu, N. Cui, Z. Yang, J. Wu, L.R. Giwa, L. Abdulkadir, P. Sharma, C. Jiang, Direct activation of cloned K_{ATP} channels by intracellular acidosis, J. Biol. Chem. 276 (2001) 12898–12902.
[11] A.P. Babenko, L. Aguilar-Bryan, J. Bryan, A view of sur/KIR6.X, K_{ATP} channels, Annu. Rev. Physiol. 60 (1998) 667–687.
[12] D. Bichet, F.A. Haass, L.Y. Jan, Merging functional studies with structures of inward-rectifier K^+ channels, Nat. Rev., Neurosci. 4 (2003) 957–967.
[13] D.A. Doyle, Structural changes during ion channel gating, Trends Neurosci. 27 (2004) 298–302.
[14] G. Yellen, The voltage-gated potassium channels and their relatives, Nature 419 (2002) 35–42.
[15] Y. Jiang, A. Lee, J. Chen, M. Cadene, B.T. Chait, R. MacKinnon, Crystal structure and mechanism of a calcium-gated potassium channel, Nature 417 (2002) 515–522.
[16] T. Jin, L. Peng, T. Mirshahi, T. Rohacs, K.W. Chan, R. Sanchez, D.E. Logothetis, The beta-gamma subunits of G proteins gate a K^+ channel by pivoted bending of a transmembrane segment, Mol. Cell 10 (2002) 469–481.
[17] A. Kuo, J.M. Gulbis, J.F. Antcliff, T. Rahman, E.D. Lowe, J. Zimmer, J. Cuthbertson, F.M. Ashcroft, T. Ezaki, D.A. Doyle, Crystal structure of the potassium channel KirBac1.1 in the closed state, Science 300 (2003) 1922–1926.
[18] H. Sackin, M. Nanazashvili, L.G. Palmer, M. Krambis, D.E. Walters, Structural locus of the pH gate in the Kir1.1 inward rectifier channel, Biophys. J. 88 (2005) 2597–2606.
[19] S. Sukharev, M. Betanzos, C.S. Chiang, H.R. Guy, The gating mechanism of the large mechanosensitive channel MscL, Nature 409 (2001) 720–724.
[20] N. Unwin, Acetylcholine receptor channel imaged in the open state, Nature 373 (1995) 37–43.
[21] N. Unwin, Structure and action of the nicotinic acetylcholine receptor explored by electron microscopy, FEBS Lett. 555 (2003) 91–95.
[22] J. Wu, H. Xu, Z. Yang, Y. Wang, J. Mao, C. Jiang, Protons activate homomeric Kir6.2 channels by selective suppression of the long and intermediate closures, J. Membr. Biol. 190 (2002) 105–116.
[23] Z. Yang, H. Xu, N. Cui, Z. Qu, S. Chanchevalap, W. Shen, C. Jiang, Biophysical and molecular mechanisms underlying the modulation of heteromeric Kir4.1–Kir5.1 channels by CO_2 and pH, J. Gen. Physiol. 116 (2000) 33–45.
[24] G. Zhu, C. Liu, Z. Qu, S. Chanchevalap, H. Xu, C. Jiang, CO(2) inhibits specific inward rectifier K^+ channels by decreases in intra- and extracellular pH, J. Cell. Physiol. 183 (2000) 53–64.
[25] J. Wu, N. Cui, H. Piao, Y. Wang, H. Xu, J. Mao, C. Jiang, Allosteric modulation of the mouse Kir6.2 channel by intracellular H^+ and ATP, J. Physiol. 543 (2002) 495–504.
[26] D. Colquhoun, A.G. Hawkes, The principles of the stochastic interpretation of ion-channel mechanisms, in: B. Sakmann, E. Neher (Eds.), Single-Channel Recording, Plenum Press, New York, 1995, pp. 397–482.
[27] S. Trapp, P. Proks, S.J. Tucker, F.M. Ashcroft, Molecular analysis of ATP-sensitive K channel gating and implications for channel inhibition by ATP, J. Gen. Physiol. 112 (1998) 333–349.
[28] D.A. Doyle, C.J. Morais, R.A. Pfuetzner, A. Kuo, J.M. Gulbis, S.L. Cohen, B.T. Chait, R. MacKinnon, The structure of the potassium channel: molecular basis of K^+ conduction and selectivity, Science 280 (1998) 69–77.
[29] P.E. Light, C. Bladen, R.J. Winkfein, M.P. Walsh, R.J. French, Molecular basis of protein kinase C-induced activation of ATP-sensitive potassium channels, Proc. Natl. Acad. Sci. U. S. A. 97 (2000) 9058–9063.
[30] Y.F. Lin, Y.N. Jan, L.Y. Jan, Regulation of ATP-sensitive potassium channel function by protein kinase A-mediated phosphorylation in transfected HEK293 cells, EMBO J. 19 (2000) 942–955.
[31] K. Tanabe, S.J. Tucker, M. Matsuo, P. Proks, F.M. Ashcroft, S. Seino, T. Amachi, K. Ueda, Direct photoaffinity labeling of the Kir6.2 subunit of the ATP-sensitive K^+ channel by 8-azido-ATP, J. Biol. Chem. 274 (1999) 3931–3933.
[32] T. Tsuboi, J.D. Lippiat, F.M. Ashcroft, G.A. Rutter, ATP-dependent interaction of the cytosolic domains of the inwardly rectifying K^+ channel Kir6.2 revealed by fluorescence resonance energy transfer, Proc. Natl. Acad. Sci. U. S. A. 101 (2004) 76–81.
[33] C.M. Armstrong, Time course of TEA^+-induced anomalous rectification in squid giant axons, J. Gen. Physiol. 273 (1966) F516–F529.
[34] G.E. Flynn, W.N. Zagotta, Conformational changes in S6 coupled to the opening of cyclic nucleotide-gated channels, Neuron 30 (2001) 689–698.
[35] J.P. Johnson Jr., W.N. Zagotta, Rotational movement during cyclic nucleotide-gated channel opening, Nature 412 (2001) 917–921.

[36] E. Perozo, D.M. Cortes, L.G. Cuello, Structural rearrangements underlying K^+-channel activation gating, Science 285 (1999) 73–78.
[37] L.R. Phillips, D. Enkvetchakul, C.G. Nichols, Gating dependence of inner pore access in inward rectifier K^+ channels, Neuron 37 (2003) 953–962.
[38] K.S. Shin, B.S. Rothberg, G. Yellen, Blocker state dependence and trapping in hyperpolarization-activated cation channels: evidence for an intracellular activation gate, J. Gen. Physiol. 117 (2001) 91–101.
[39] C.E. Capener, I.H. Shrivastava, K.M. Ranatunga, L.R. Forrest, G.R. Smith, M.S. Sansom, Homology modeling and molecular dynamics simulation studies of an inward rectifier potassium channel, Biophys. J. 78 (2000) 2929–2942.
[40] J. Kyte, R.F. Doolittle, A simple method for displaying the hydropathic character of a protein, J. Mol. Biol. 157 (1982) 105–132.
[41] W.C. Wimley, S.H. White, Experimentally determined hydrophobicity scale for proteins at membrane interfaces, Nat. Struct. Biol. 3 (1996) 842–848.
[42] S.H. White, W.C. Wimley, Membrane protein folding and stability: physical principles, Annu. Rev. Biophys. Biomol. Struct. 28 (1999) 319–365.